Peak floor acceleration prediction using spectral shape: Comparison between acceleration and velocity

José I. Torres[1], Edén Bojórquez[*], Robespierre Chavez[**1], Juan Bojórquez[***1], Alfredo Reyes-Salazar[1], Víctor Baca[****1], Federico Valenzuela[1], Joel Carvajal[1], Omar Payán[2] and Martín Leal[1]

[1]Facultad de Ingeniería, Universidad Autónoma de Sinaloa, Calzada de las Américas y B. Universitarios s/n, C.P. 80040, Culiacán, Sinaloa, México
2Department of Mechanical and Mechatronic Engineering, Tecnológico Nacional de México Campus Culiacán, Culiacán, Sinaloa, México

Abstract. In this study, the generalized intensity measure (IM) named I_{Npg} is analyzed. The recently proposed proxy of the spectral shape named N_{pg} is the base of this intensity measure, which is similar to the traditional N_p based on the spectral shape in terms of pseudo-acceleration; however, in this case the new generalized intensity measure can be defined through other types of spectral shapes such as those obtained with velocity, displacement, input energy, inelastic parameters and so on. It is shown that this IM is able to increase the efficiency in the prediction of nonlinear behavior of structures subjected to earthquake ground motions. For this work, the efficiency of two particular cases (based on acceleration and velocity) of the generalized I_{Npg} to predict the peak floor acceleration demands on steel frames under 30 earthquake ground motions with respect to the traditional spectral acceleration at first mode of vibration $Sa(T_1)$ is compared. Additionally, a 3D reinforced concrete building and an irregular steel frame is used as a basis for comparison. It is concluded that the use of velocity and acceleration spectral shape increase the efficiency to predict peak floor accelerations in comparison with the traditional and most used around the world spectral acceleration at first mode of vibration.

Keywords: efficiency; intensity measure; peak floor acceleration; seismic response; spectral shape

1. Introduction

Several efforts have been focused to find an efficient intensity measure able to reduce the uncertainty of the structural response of buildings under several earthquake ground motions. The efficiency is defined as the ability to reduce the uncertainty of the seismic response of structures subjected to earthquakes. The literature shows that several studies have been developed with the aim to observe the relation between intensity measures and the seismic response of structures, and various intensity measures have been proposed or analyzed (Housner 1952, Housner 1975, Arias 1970, Aptikaev 1982, Von-Thun *et al.* 1988, Cordova *et al.* 2001, Shome 1999, Tothong 2007, Riddell 2007, Mehanny 2009, Bojórquez and Iervolino 2011, Bojórquez *et al.* 2012, Minas *et al.* 2014, Kostinakis *et al.* 2015, Yakhchalian *et al.* 2015, Kazantzi and Vamvatsikos 2015). Currently, several studies promote the use of vector-valued or scalar ground motion IMs based on spectral shape,

because they predict with good accuracy the maximum inter-story drift of buildings subjected to earthquakes (Bojórquez and Iervolino 2011, 2012). Furthermore, vector and scalar ground motion intensity measures based on N_p which are representative of the spectral shape have resulted very well related with the nonlinear structural response in terms of peak and energy demands (Bojórquez and Iervolino 2011, Bojórquez *et al.* 2012, Minas *et al.* 2014, Buratti 2012, Modica and Stafford 2014, Malaga-Chuquitaype and Bougatsas 2017, Rajabnejad *et al.* 2021). In addition, N_p has been successfully used for record selection (Bojórquez *et al.* 2013). The ground motion intensity measure (Bojórquez and Iervolino 2011) based on the spectral parameter of pseudo-acceleration has demonstrated to be one of the most efficient (Buratti 2012, Rajabnejad *et al.* 2021). Moreover, with the aim to improve the predictive capacity of I_{Np}, Bojórquez *et al.* (2017) proposed the generalized intensity measure I_{Npg}, based on the generalized spectral shape parameter N_{pg}, where any parameter of spectral shape can be used. Nevertheless, most of the studies to illustrate the potential of N_p-based intensity measures are related to the spectral shape in terms of acceleration where only the standard deviation of the maximum inter-story drift has been analyzed. Thus, it is necessary to estimate the relation between intensity measures and maximum responses using some other spectral parameter as in the case of velocity which is related with energy. In general, most of the studies that propose new intensity measures used the maximum displacement or inter-story drift to analyze the IM's efficiency; however,

---

∗Corresponding author, Professor
  E-mail: eden@uas.edu.mx
∗∗Ph.D.
  E-mail: robespierre@uas.edu.mx
∗∗∗Professor
  E-mail: juanbm@uas.edu.mx
∗∗∗∗Professor
  E-mail: victor02305@hotmail.com

other important parameter that must be taken into account to avoid the damage in nonstructural components such as hospital equipment is the peak floor acceleration as it has been demonstrated in several studies (Kehoe and Freeman 1998, Horne and Burton 2003). In such a way that it is important to develop more studies of efficiency to estimate peak floor accelerations demands in order to analyze the predictive ability of the most used ground motion intensity measures $Sa(T_1)$ in comparison with other IM's such as I_{Npg}. Therefore, in this work an efficiency study of the generalized I_{Npg} ground motion intensity measure based on peak floor accelerations and using as spectral parameters the pseudo-acceleration and velocity is performed. The aim of this study is to demonstrate a better efficiency of I_{Npg} in the prediction of the structural response in terms of peak floor accelerations of multi-story buildings than the commonly used spectral acceleration at first mode of vibration.

2. The origin of the generalized spectral shape parameter N_{pg} and selected intensity measures

Several studies suggest that the spectral shape is crucial to predict the structural response of buildings under earthquakes and for this reason the earthquake engineering and seismology community has highlighted the limitations of spectral acceleration at first mode of vibration $Sa(T_1)$. For example, it has been shown that $Sa(T_1)$ does not provide information about the spectral shape in other regions of the spectrum, which may be important for the nonlinear behavior beyond first mode of vibration T_1, or for structures dominated by higher modes (periods smaller than T_1). In the case of nonlinear shaking, the structure may be sensitive to different spectral values associated to a range of periods defined, from the fundamental period and a limit value of practical interest, say T_N. For this reason, Bojórquez and Iervolino (2011) proposed a spectral shape parameter named N_p. It is important to say that the traditional N_p can be generalized to account for higher mode effects as (Bojórquez *et al.* 2011, 2015) recommend. For example, (Bojórquez *et al.* 2013) used the parameter N_p to account for higher mode effects in order to propose a new spectral shape-based record selection approach using genetic algorithms. Furthermore, (Bojórquez *et al.* 2011, 2015) indicates that N_p can be calculated using a different range of periods. In general, Bojórquez *et al.* (2013) indicates that the higher mode effects can be incorporated by modifying the parameter N_p evaluating not only from the period T_1 up to T_N but also from the period of some mode of interest (a period smaller than T_1) until the final period T_N (Bojórquez *et al.* 2017). For example, with the assessment of N_p from T_{2mode} up to T_N (T_{2mode} is the period associated to the second mode of vibration of the structure). Moreover, instead of spectral acceleration other spectral shape parameters could be used. A generalized N_{pg} can be written as follows:

$$N_{pg} = \frac{S_{avg}(T_i,...,T_N)}{S(T_j)} \tag{1}$$

In Eq. (1), $S(T_j)$ represents a spectral parameter taken from any type of spectrum at period T_j as in the case of acceleration, velocity, displacement, input energy, inelastic parameters and so on. $Sa_{avg}(T_i,...,T_N)$ is the geometrical mean of a specific spectral parameter between the range of periods T_i and T_N. Note that the periods T_i and T_j could be different; N_{pg} is similar to the traditional definition of N_p (Bojórquez and Iervolino 2011) but for different types of spectra and a wider range of periods. In such a way that parameters as the traditional N_p or the recently proposed $SaRatio$ (Eads *et al.* 2016) are particular cases of the generalized spectral shape parameter N_{pg}. If the pseudo-acceleration spectrum is used, and $T_i=T_j=T_1$ (first mode structural vibration period) N_{pg} is equals to the traditional N_p and can also be shown as N_{pSa}, and it is expressed as follows:

$$N_{pg} = N_{pSa} = \frac{Sa_{avg}(T_1,...,T_N)}{Sa(T_1)} \tag{2}$$

Similarly, if the velocity spectrum is used, and $T_i=T_j=T_1$ N_{pg} is equal to N_{pVel} is expressed as follows:

$$N_{pVel} = \frac{Vel_{avg}(T_1,...,T_N)}{Vel(T_1)} \tag{3}$$

The information given by the traditional N_p equation is that if we have one or n records with a mean N_p value close to one, we can expect an average spectrum near flat in the period range between T_1 and T_N. For a mean N_p lower than one, it is expected an average spectrum with a negative slope. In the case of N_{pg} values, the information provided on the average spectrum in the range between T_1 and T_N indicates the same as for the values of N_p, regardless of the spectral parameter that is being used. Notice that in Eqs. (2)-(3) the subscripts indicate the spectral parameter selected, for example, in Eq. (2) the subscript Sa after N_p indicates that pseudo acceleration is being used as a spectral parameter. As an example, the mean value of N_{pSa} for a group of ordinary records in the period range $T_1 = 0.6$s to $T_N = 2T_1$ is 0.32. In Fig. 1(a), the average spectrum of this set is illustrated. In the case of N_{pSa} values larger than one, the spectra tend to increase beyond T_1. As it can be appreciated for a set of narrow-band records, where the mean value of $N_p = 1.8$ for $T_1 = 1.2$s and $T_N = 2T_1$, the average spectrum shows an increasing accelerations zone (see Fig. 1(b)).

In the case that velocity is used as a spectral parameter (see Fig. 2), if the N_{pg} values are close to one, the spectrum tends to be flat between T_1 and T_N, that is illustrated in Fig. 2(a) for the set of ordinary records, where the average value of $N_{pVel}=0.95$ for $T_1=1.2$s and $T_N=2.4$s, the average spectrum shows that the velocities are similar in the considered zone. The average spectrum for the set of narrow-band record is shown in Fig. 2(b), where the mean value of N_{pVel} in the period range $T_1=1.2$ to $T_N=2T_1$ is 1.44, then it can be observed that for larger N_{pg} values than one, regardless of the spectral parameter used, the spectra tend to increase beyond T_1.

Finally, as it was stated before, the initial period T_1 and the final period T_N in the N_{pg} parameter can be changed to
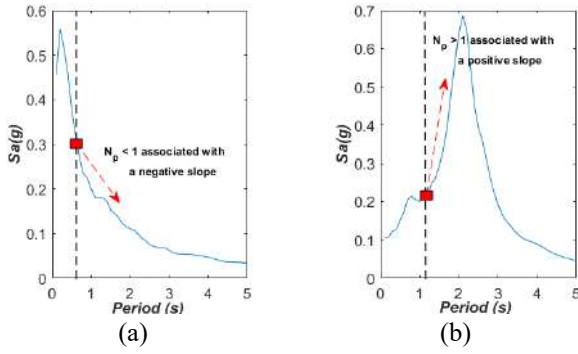
Fig. 1 Mean elastic response spectra for a set of: (a) ordinary records with $N_p = 0.32$, (b) narrow-band records with $N_p = 1.8$
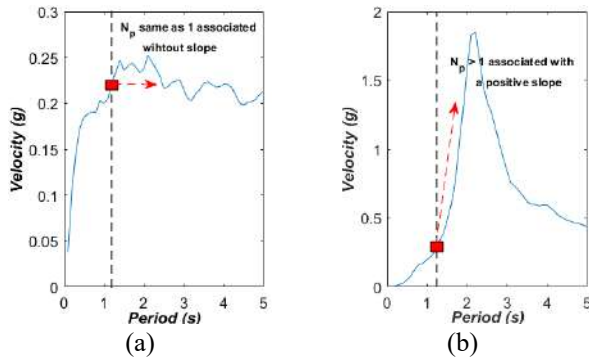

Fig. 2 Mean elastic response spectra for a set of: (a) ordinary records with $N_p = 0.95$, (b) narrow-band records with $N_p = 1.44$.

Table 1 Characteristics of the structural steel frame models

Frame	Number of stories	Period of vibration (s) T_1	C_y
F4	4	0.90	0.45
F6	6	1.07	0.42
F8	8	1.20	0.38
F10	10	1.35	0.36
F14	14	1.91	0.25
F18	18	2.53	0.185
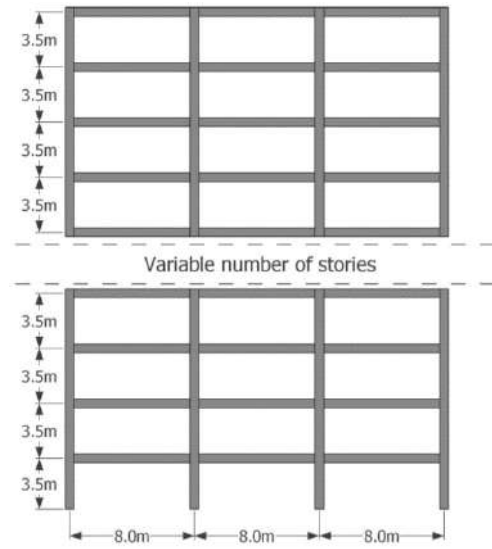
Fig. 3 Geometrical characteristics of the steel frames

account for higher mode effects as demonstrated by Bojórquez *et al*. (2011), (2013), (2015). Hence, N_{pg} is not limited to a specific range and the spectral parameter can be taken from any response spectrum demand such as velocity, displacement, seismic energy, etc. as it was previously suggested by Bojórquez *et al*. (2011), (2015).

The generalized I_{Npg} (Bojórquez *et al*. 2017) can be defined as follows:

$$I_{Npg} = S(T_1) N_{pg}{}^{\alpha} \qquad (4)$$

In Eq. (4) the α value has to be determined from regression analysis, $S(T_1)$ represents a spectral parameter taken from any type of spectrum as in the case of acceleration, velocity, displacement, input energy, inelastic parameters and so on, at first mode of vibration. The generalized N_{pg} is defined in Eq. (1). In this study only pseudo-acceleration and velocity spectral parameters are considered, therefore, when these parameters are substituted in Eq. (4), the following equations are obtained:

$$I_{NpSa} = Sa(T_1) \frac{Sa_{avg}(T_1,...,T_N)^{\alpha}}{Sa(T_1)} \qquad (5)$$

$$I_{NpVel} = Vel(T_1) \frac{Vel_{avg}(T_1,...,T_N)^{\alpha}}{Vel(T_1)} \qquad (6)$$

Note that in Eqs. (5)-(6) the subscripts indicate the spectral parameter used, for example, in Eq. (6) the subscript *Vel* after I_{Np} indicates that velocity is being used as a spectral parameter. From Eq. (5), it is possible to note that when pseudo-acceleration is used: 1) the traditional intensity measure I_{Np} proposed by Bojórquez and Iervolino (2011) is a particular case of the generalized I_{Npg}; 2) the spectral acceleration at first mode of vibration is a particular case, and this occurs when α is equal to zero; 3) $Sa_{avg}(T_1...T^N)$ also corresponds to the particular case when α = 1. Analyses developed by Bojórquez and Iervolino and others (Bojórquez and Iervolino 2011, Buratti 2012) suggest that the optimal values of α are close to 0.4 for the traditional I_{Np} or I_{NpSa}. Furthermore, Buratti (2012) demonstrated that this intensity measure is more efficient to predict the seismic response of structures compared with several intensity measures existing in the literature. In the present work, the efficiency of $Sa(T_1)$, I_{NpSa} and I_{NpVel} to predict peak floor accelerations of structural steel frames is computed considering the α value recommend by Bojórquez and Iervolino (2011).

3. Structural steel framed buildings

The efficiency of the selected two particular cases of I_{Npg} based on acceleration and velocity is estimated using six moment-resisting steel frames having 4, 6, 8, 10, 14 and 18 stories. The frames represent typical steel buildings in

Table 2 Summary of the column sizes of the steel frames

Frame	F4	F6	F8	F10	F14	F18
Number of Stories	4	6	8	10	14	18
Internal Columns						
Story 1	W21×122	W30×173	W36×210	W36×280	W36×328	W36×359
Story 2	W21×122	W30×173	W36×210	W36×280	W36×328	W36×359
Story 3	W21×111	W30×148	W36×194	W36×245	W36×280	W36×359
Story 4	W21×111	W30×148	W36×194	W36×245	W36×280	W36×359
Story 5		W30×124	W36×170	W36×210	W36×280	W36×328
Story 6		W30×124	W36×170	W36×210	W36×280	W36×328
Story 7			W36×160	W36×182	W36×245	W36×280
Story 8			W36×160	W36×182	W36×245	W36×280
Story 9				W36×150	W36×210	W36×245
Story 10				W36×150	W36×210	W36×245
Story 11					W36×182	W36×210
Story 12					W36×182	W36×210
Story 13					W36×150	W36×182
Story 14					W36×150	W36×182
Story 15						W36×150
Story 16						W36×150
Story 17						W36×150
Story 18						W36×150
External Columns						
Story 1	W18×97	W27×146	W36×194	W36×280	W36×328	W36×359
Story 2	W18×97	W27×146	W36×194	W36×280	W36×328	W36×359
Story 3	W18×86	W27×129	W36×182	W36×245	W36×280	W36×359
Story 4	W18×86	W27×129	W36×182	W36×245	W36×280	W36×359
Story 5		W27×114	W36×160	W36×210	W36×280	W36×328
Story 6		W27×114	W36×160	W36×210	W36×280	W36×328
Story 7			W36×135	W36×182	W36×245	W36×280
Story 8			W36×135	W36×182	W36×245	W36×280
Story 9				W36×150	W36×210	W36×245
Story 10				W36×150	W36×210	W36×245
Story 11					W36×182	W36×210
Story 12					W36×182	W36×210
Story 13					W36×150	W36×182
Story 14					W36×150	W36×182
Story 15						W36×150
Story 16						W36×150
Story 17						W36×150
Story 18						W36×150

Mexico, and they were designed in accordance with the Mexico City Building Code, they have three eight-meter bays and story heights of 3.5 m. For the dynamic analysis of the steel frames models, the RUAUMOKO program Carr, (2011) was used. The dynamic characteristics for each frame, such as the structural vibration period (T_l) and the seismic coefficient (C_y) are shown in Table 1 (the latter value was established from static nonlinear analyses). In addition, Tables 2-3 illustrate more details about the selected steel frames. An elasto-plastic model with 3% strain-hardening was used to represent the hysteretic behavior of the steel beams and columns, and 3% of critical damping was assumed to the first two modes of vibration of the frames. The geometric characteristics of the structures are illustrated in Fig. 3. More information of the selected structural steel models can be seen in Bojórquez *et al.* (2010).

4. Ground motion records

30 narrow-banded ground motions recorded at soft soil sites of Mexico City have been selected for nonlinear dynamic analysis. The most important characteristics of the records are summarized in Table 4. It should be mentioned that soft soil sites are very common in Mexico City and that the higher levels of shaking (in terms of peak ground acceleration *PGA* and velocity *PGV*) have been consistently observed at these sites. Moreover, most of the structural damages in the well-known 1985 Mexican earthquake occurred in the selected sites.

5. Incremental dynamic analysis

The efficiency of I_{NpSa} and I_{NpVel} for the estimation of

Table 3 Summary of the beam sizes of the steel frames

Frame	F4	F6	F8	F10	F14	F18
Number of Stories	4	6	8	10	14	18
Beams						
Story 1	W16×67	W18×71	W21×83	W21×68	W21×93	W21×101
Story 2	W16×57	W18×76	W21×93	W21×93	W21×93	W21×101
Story 3	W16×45	W18×76	W21×93	W21×101	W21×111	W21×111
Story 4	W16×40	W16×67	W21×83	W21×101	W21×111	W21×111
Story 5		W16×50	W18×71	W21×101	W21×111	W21×111
Story 6		W16×45	W18×65	W21×93	W21×101	W21×101
Story 7			W18×55	W21×73	W21×93	W21×101
Story 8			W18×46	W21×68	W21×83	W21×93
Story 9				W21×57	W21×83	W21×93
Story 10				W21×50	W21×73	W21×83
Story 11					W21×73	W21×83
Story 12					W21×62	W21×73
Story 13					W21×62	W21×73
Story 14					W21×57	W21×62
Story 15						W21×62
Story 16						W21×62
Story 17						W21×57
Story 18						W21×57

Table 4 Narrow-band earthquake ground motions

Rec.	Date	Magnitude	PGA (cm/s²)	PGV (cm/s)	Duration (s)
1	19/09/1985	8.1	178.0	59.5	34.8
2	21/09/1985	7.6	48.7	14.6	39.9
3	25/04/1989	6.9	45.0	15.6	37.8
4	25/04/1989	6.9	68.0	21.5	65.5
5	25/04/1989	6.9	44.9	12.8	65.8
6	25/04/1989	6.9	45.1	15.3	79.4
7	25/04/1989	6.9	52.9	17.3	56.6
8	25/04/1989	6.9	49.5	17.3	50.0
9	14/09/1995	7.3	39.3	12.2	53.7
10	14/09/1995	7.3	39.1	10.6	86.8
11	14/09/1995	7.3	30.1	9.62	60.0
12	14/09/1995	7.3	33.5	9.37	77.8
13	14/09/1995	7.3	34.3	12.5	101.2
14	14/09/1995	7.3	27.5	7.8	85.9
15	14/09/1995	7.3	27.2	7.4	68.3
16	09/10/1995	7.5	14.4	4.6	85.5
17	09/10/1995	7.5	15.8	5.1	97.6
18	09/10/1995	7.5	15.7	4.8	82.6
19	09/10/1995	7.5	24.9	8.6	105.1
20	09/10/1995	7.5	17.6	6.3	104.5
21	09/10/1995	7.5	19.2	7.9	137.5
22	09/10/1995	7.5	13.7	5.3	98.4
23	09/10/1995	7.5	17.9	7.18	62.3
24	11/01/1997	6.9	16.2	5.9	61.1
25	11/01/1997	6.9	16.3	5.5	85.7
26	11/01/1997	6.9	18.7	6.9	57.0
27	11/01/1997	6.9	22.2	8.6	76.7
28	11/01/1997	6.9	21.0	7.76	74.1
29	11/01/1997	6.9	20.4	7.1	81.6
30	11/01/1997	6.9	16.0	7.2	57.5

peak floor acceleration demands of the selected steel frames under narrow-band motions in comparison with $Sa(T_1)$ is

estimated thought incremental dynamic analysis (Vamvatsikos and Cornell 2002). For this aim, the records are scaled at different $Sa(T_1)$, I_{NpSa} and I_{NpVel} values, in order to show the uncertainty in the prediction of peak floor accelerations. A couple of examples of the scaling process can be seen in Figs. 4 and 5, where Fig. 4 illustrates the response spectra of the intensity measure I_{NpSa} scaled for an intensity of 0.5g at the fundamental period of the steel Frame F8 (T_1=1.2 s) for the selected seismic records. In addition, Fig. 5 shows the response spectra of the intensity measure I_{NpVel} at the fundamental period of the steel Frame F14 (T_1=1.91 s) of the selected seismic records scaled at 0.3 cm/s. It is worth mentioning that in this study is the first time that this type of spectrum (velocity) is used to define the spectral shape parameter N_p.

As it was mentioned before, the computer program RUAUMOKO was used to complete a total of 8640 non-linear structural dynamic analyzes in order to assess the peak floor acceleration demands of each structure. Fig. 6 illustrate a typical plot of incremental dynamic analysis results for $Sa(T_1)$ in terms of peak floor accelerations calculated for the frames models F4, F6, F8, F10, F14 and F18 under the selected narrow-band motions. It is observed a clear relation between peak floor acceleration and $Sa(T_1)$ for low levels of intensities of the earthquake ground motions; however, the uncertainty to predict peaks demands using the spectral acceleration tends to increase as the intensity raises. For this reason, it is necessary to use promising intensity measures with better prediction capacity of the structural response as in the case of the generalized I_{Npg}. It is appreciated in Fig. 6 that for $Sa(T_1)$ values smaller than 0.5 g, spectral acceleration is an excellent candidate as intensity measure since the uncertainty in the prediction is despicable; in fact, the seismic response of the steel structure is almost linear elastic. Nevertheless, for values of intensities equals to 1.6 g, the peak floor acceleration
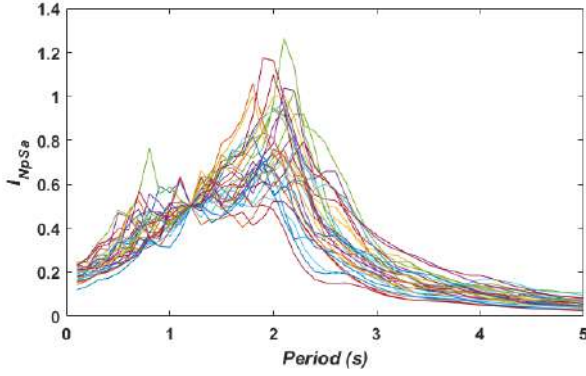
Fig. 4 Response spectra of the intensity measure I_{NpSa} scaled at an intensity of 0.5 g in the fundamental period of the steel Frame F8 (T_I=1.2 s) for the selected seismic records
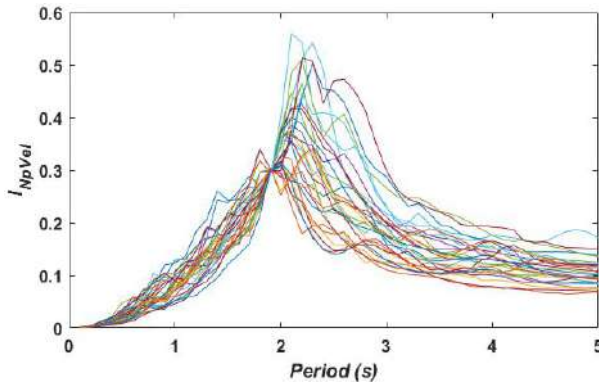

Fig. 5 Response spectra of the intensity measure I_{NpVel} scaled at an intensity of 0.3 cm/s in the fundamental period of the steel Frame F14 (T_I=1.91 s) for the selected seismic records

demands are in the range of 7 m/s2 up to 19 m/s2, which indicate large uncertainty and the limitations of $Sa(T_I)$ to predict the seismic response of this structure for large levels of nonlinear behavior. On the other hand, in Fig. 7 incremental dynamic analysis for the six steel frames is illustrated, in which the vertical axis corresponds to the peak floor acceleration and the horizontal to the records scaled at different I_{NpSa} values. From Fig. 7, it can be seen that for low level of intensity values, I_{NpSa} is an excellent predictor of the structural response. Moreover, for large values of intensities, the range of peak floor acceleration demands at a specific level of I_{NpSa} is not so large as in the case of $Sa(T_I)$. For example, the range of peak floor acceleration is from 6 m/s2 until 18 m/s2 for I_{NpSa} values of 1.6 g, indicating the advantages of using the intensity measure I_{NpSa} in comparison with the spectral acceleration at first mode of vibration. Similar results are observed in the case of I_{NpVel} as can be appreciated in Fig. 8. In general, it is observed that large uncertainty is associated with the spectral acceleration as intensity measure. Thus, the generalized intensity measure I_{Npg} could characterize with better efficiency the seismic response of buildings under narrow-band motions in terms of peak floor accelerations, at least for the selected steel framed buildings. This issue will be better discussed in the next section.
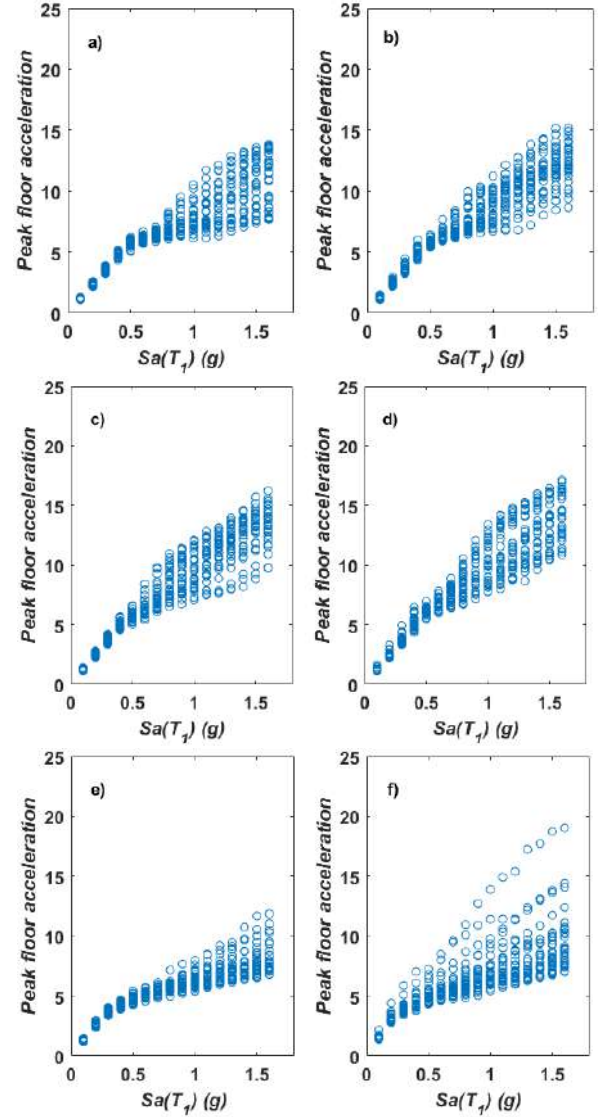

Fig. 6 Incremental dynamic analysis for the selected steel Frames under narrow-band motions using $Sa(T_I)$ as intensity measure: (a) F4, (b) F6, (c) F8, (d) F10, (e) F14, (f) F18

6. Efficiency study

From the dynamic analyses performed in the previous chapter, the peak floor accelerations for each structure and all intensity measures considered in the study have been obtained. Then the standard deviation of the natural logarithm of the peak floor acceleration for the six steel frames and each intensity level has been computed, which is illustrated in Figs. 9-11. In these figures, the horizontal axes represent the intensity level and the steel frames under consideration, and the vertical axis represents the standard deviation of the natural logarithm of the peak floor accelerations. Although the figures illustrate that the standard deviation seems smaller for the two particular cases of I_{Npg} in comparison with $Sa(T_I)$. Notice that a direct comparison cannot be made for a similar level of intensity in terms of I_{NpSa}, I_{NpVel} and $Sa(T_I)$. Nevertheless, the figures let conclude that the uncertainty tend to increase as the
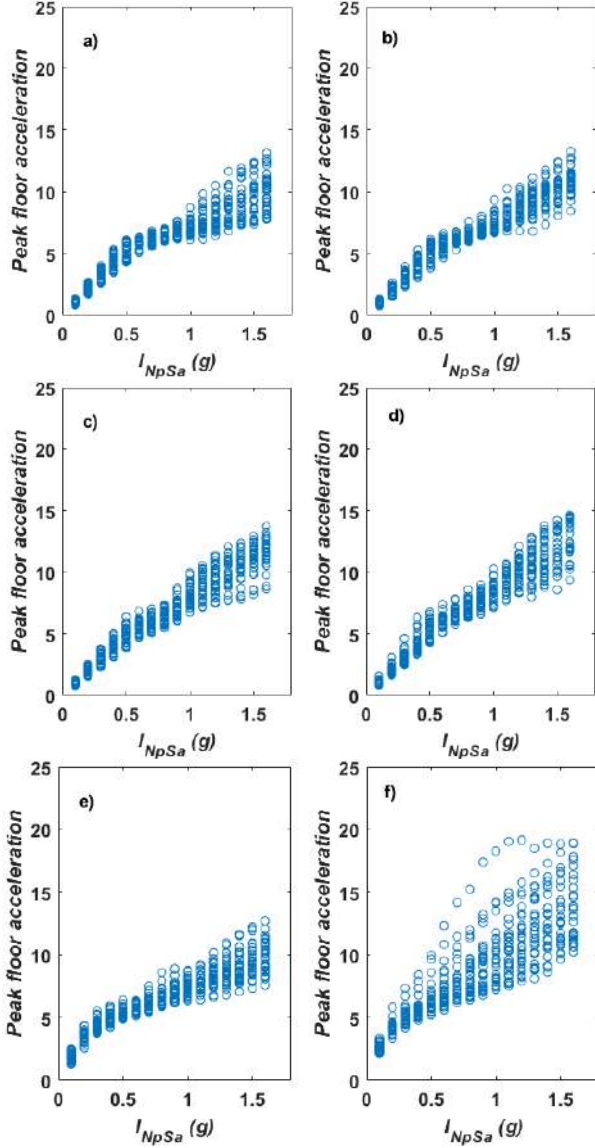
Fig. 7 Incremental dynamic analysis for the selected steel Frames under narrow-band motions using I_{NpSa} as intensity measure: (a) F4, (b) F6, (c) F8, (d) F10, (e) F14, (f) F18
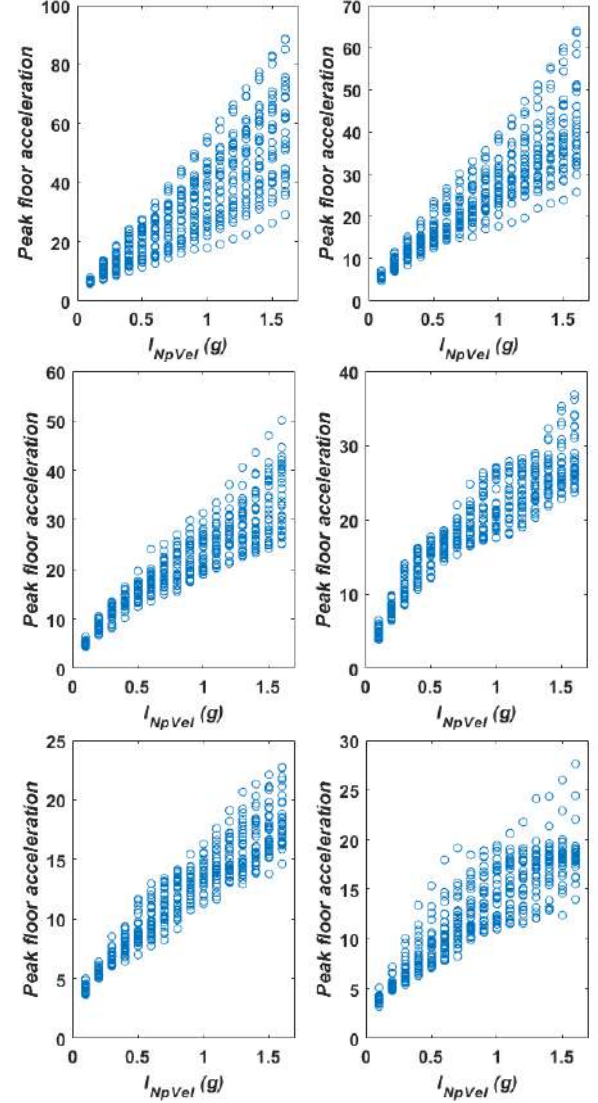

Fig. 8 Incremental dynamic analysis for the selected steel Frames under narrow-band motions using I_{NpVel} as intensity measure:(a) F4, (b) F6, (c) F8, (d) F10, (e) F14, (f) F18

number of story levels increases. This conclusion is valid for all the selected spectral shape parameter as intensity measure. In the case of the I_{NpVel} uncertainty of low-rise buildings is considerably similar in comparison with tall buildings. In order to develop a fair comparison among the selected intensity measures, it is necessary to obtain the standard deviation of the natural logarithm of the peak floor acceleration for a specific performance level as it is shown below.

To illustrate the potential of I_{NpSa} and I_{NpVel} in the prediction of the structural response, a scaling level of 1.6 g for $Sa(T_1)$, 1.6 g for I_{NpSa} and 1.6 cm/s for I_{NpVel} are considered, it can be seen in Figs. 6-8 that for I_{NpSa} and $Sa(T_1)$ the demands of peak floor acceleration are similar, on the other hand, in the case of I_{NpVel} the demands of peak floor acceleration increase considerably, however, if the standard deviations shown in Figs. 9-11 for the six steel frames at the intensities mentioned above are compared, it
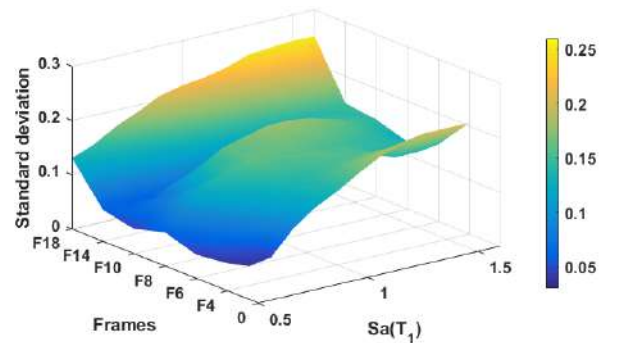

Fig. 9 Standard deviation of peak floor acceleration in the case of $Sa(T_1)$ for all the steel frames

is observed that the efficiency of I_{NpSa} and I_{NpVel} is similar, with an average standard deviation of 0.13 and 0.14 respectively, for the case of $Sa(T_1)$ its limited efficiency is evidenced by obtaining an average standard deviation of 0.17.
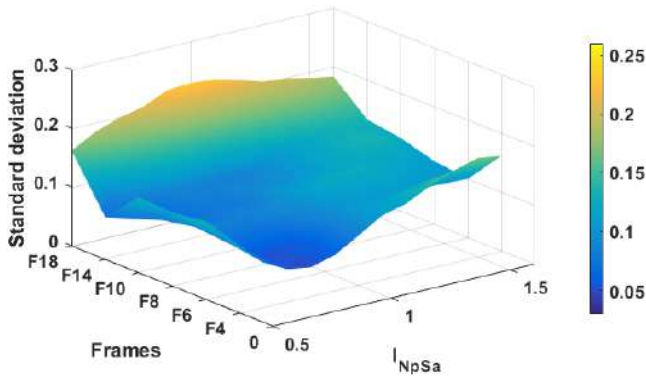
Fig. 10 Standard deviation of peak floor acceleration in the case of the generalized intensity measure I_{NpSa} for all the steel frames
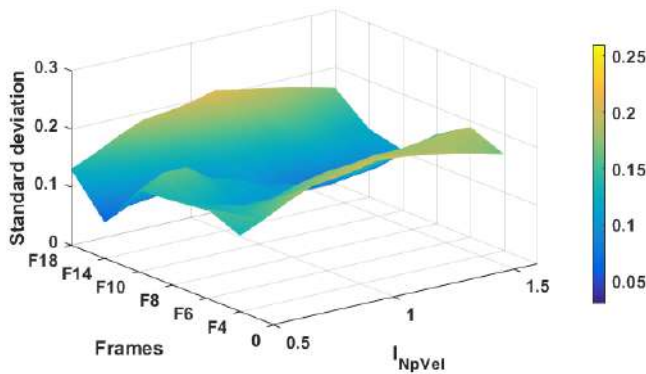

Fig. 11 Standard deviation of peak floor acceleration in the case of the generalized intensity measure I_{NpVel} for all the steel frames

Fig. 12 Standard deviation of the peak floor acceleration of the two cases of the generalized intensity measure I_{Npg} and $Sa(T_1)$ at different median values of the peak floor acceleration for the steel Frame F4

Fig. 13 Standard deviation of the peak floor acceleration of the two cases of the generalized intensity measure I_{Npg} and $Sa(T_1)$ at different median values of the peak floor acceleration for the steel Frame F6

Fig. 14 Standard deviation of the peak floor acceleration of the two cases of the generalized intensity measure I_{Npg} and $Sa(T_1)$ at different median values of the peak floor acceleration for the steel Frame F8

As it was stated, the above comparison is not entirely fair, but gives an idea of the efficiency of I_{NpSa} and I_{NpVel} in the prediction of structural response. In this part of the study, a comparison is provided but considering the same level of structural demand. Therefore, to evaluate the efficiency of the two particular cases of generalized intensity measure I_{Npg} defined with Eqs. (5)-(6), the median peak floor acceleration and the standard deviation of the natural logarithm of the peak floor acceleration of the buildings under the set of narrow-band earthquake ground motions were computed for each scaling value. Figs. 12-17 shows the results of the standard deviation of the peak floor acceleration for the two cases of the generalized intensity measure I_{Npg} (using pseudo-acceleration and velocity as spectral parameters) and $Sa(T_1)$ at a specific median value of the peak floor acceleration for the narrow-band motions and the steel Frames F4, F6, F8, F10, F14 and F18, where the vertical axis corresponds to the standard deviation of the peak floor acceleration, and the horizontal to the median peak floor acceleration value.

The results for the low-rise steel frames are plotted in Figs. 12-13. From Fig. 12 it can be seen that for the steel Frame F4, the intensity measure I_{NpVel} has lower standard deviation for most of the median peak floor acceleration values. Notice that the intensity measure with the highest standard deviation for most of the median peak floor
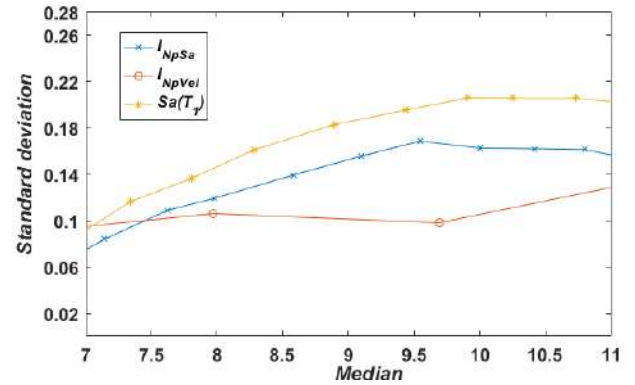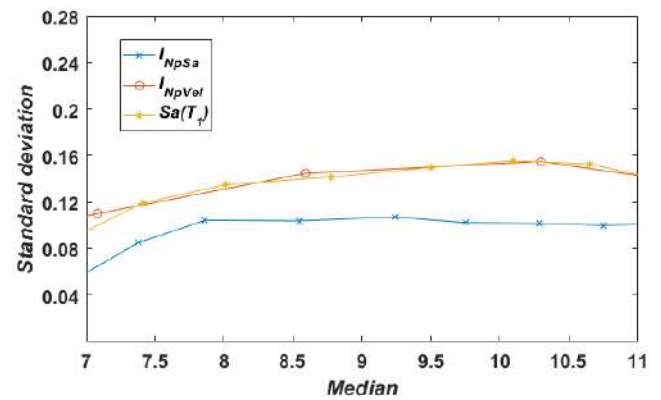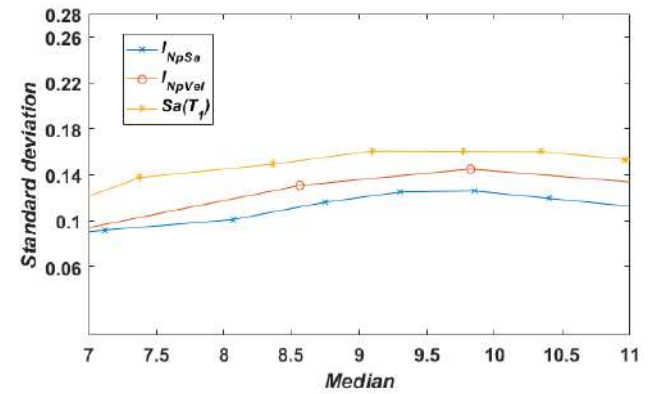
acceleration values is $Sa(T_1)$. While for the steel Frame F6 (Fig. 13) the intensity measure I_{NpSa} presents lower standard deviation of the peak floor acceleration for all of the median values; therefore, for low-rise steel frames with T_1 less than 1.1s it could be used either one of the two particular cases of the generalized intensity measure I_{Npg} to predict the structural response.
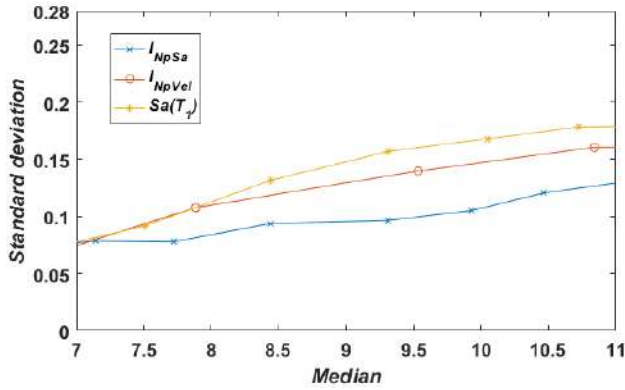
Fig. 15 Standard deviation of the peak floor acceleration of the two cases of the generalized intensity measure I_{Npg} and $Sa(T_1)$ at different median values of the peak floor acceleration for the steel Frame F10
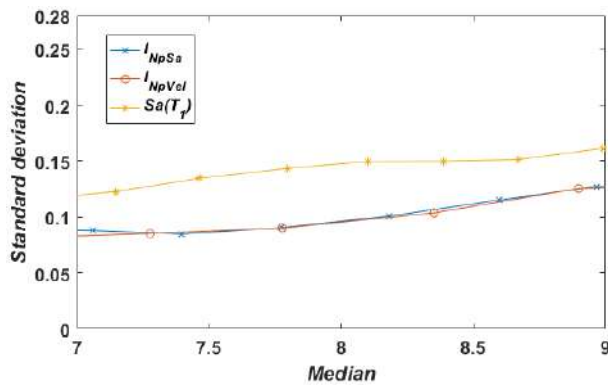

Fig. 16 Standard deviation of the peak floor acceleration of the two cases of the generalized intensity measure I_{Npg} and $Sa(T_1)$ at different median values of the peak floor acceleration for the steel Frame F14
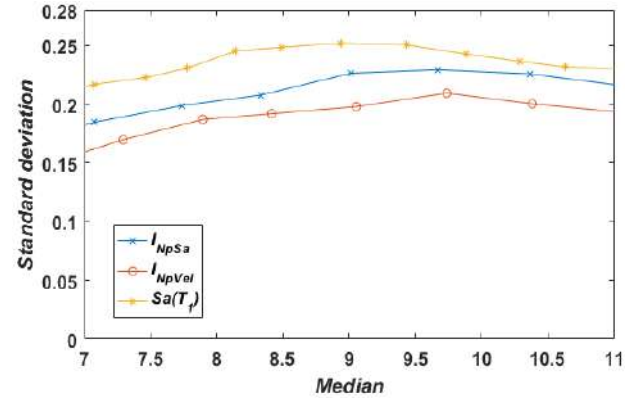

Fig. 17 Standard deviation of the peak floor acceleration of the two cases of the generalized intensity measure I_{Npg} and $Sa(T_1)$ at different median values of the peak floor acceleration for the steel Frame F18

Table 5 Comparison of the standard deviation for a median value of peak floor acceleration equals 9 m/s² and the selected intensity measures

Frames	Standard Deviation			Ratio of Standard Deviation		
	$Sa(T_1)$	I_{NpSa}	I_{NpVel}	I_{NpSa} / $Sa(T_1)$	I_{NpVel} / $Sa(T_1)$	I_{NpSa} / I_{NpVel}
F4	0.18	0.16	0.10	0.85	0.54	1.59
F6	0.14	0.11	0.13	0.76	0.93	0.74
F8	0.16	0.12	0.14	0.78	0.90	0.86
F10	0.16	0.10	0.14	0.61	0.89	0.69
F14	0.16	0.13	0.13	0.79	0.80	0.99
F18	0.25	0.23	0.20	0.90	0.79	1.14

For the steel frames F8 and F10 (Figs. 14-15), it is illustrated that the intensity measure I_{NpSa} for median peak floor acceleration values larger than 7 m/s² is more efficient because it presents less standard deviation. In this case, similarly to the low-rise steel frames, either of the two particular cases of generalized intensity measure I_{Npg} to predict the structural response could be good candidates as intensity measure, especially I_{NpSa}.

When high-rise steel frames F14 and F18 are used for the study of efficiency it can be seen that the intensity measure I_{NpVel} is the best candidate to predict the structural response (Figs. 16-17). In Fig. 16 it is shown that for most of the median peak floor acceleration values the standard deviation for both cases of I_{Npg} are very similar and less than $Sa(T_1)$. For the highest building in this study (steel frame F18) the standard deviation for the intensity measure I_{NpVel} is lower for all of the median peak floor acceleration values; on the other hand, $Sa(T_1)$ has the highest standard deviation for most of the median peak floor acceleration values (Fig. 17).

In general, for all the analyses developed, it can be seen that, for low-rise and mid-rise steel frames (smaller than 14 stories), either of the two cases of the generalized intensity measure I_{Npg} can be used for the prediction of the structural response. Further, in Figs. 12-17 it is also shown that when the height of the frames increases the efficiency of I_{NpVel} also increases, therefore, when using high-rise steel Frames (>14 stories), the ground motion intensity measure I_{NpVel} is preliminary more efficient because their standard deviations of peak floor acceleration are less than the standard deviations obtained with I_{NpSa}; nevertheless, in general the stability in the prediction of peak floor accelerations in the case of I_{NpSa} for all type of buildings is superior as it can be observed in Table 5. Perhaps, the last conclusion could be related to the fact that the vibration periods of the highest structures are near to the soil period, range where the structures are more sensitive to the velocity and energy (Riddell 2007). In this table, the standard deviation for a median value of peak floor acceleration equals 9 m/s² is computed. Furthermore, the ratio of standard deviation among the selected intensity measures also is presented. It is notice that when using I_{NpSa} or I_{NpVel} the uncertainty can be reduced up to 40% in comparison with the traditional $Sa(T_1)$. In addition, for the frames F6, F8, F10 I_{NpSa} is better predictor in comparison with I_{NpVel}, while for the structures F4 and F18, the parameter based on velocity is more efficient. Finally, although I_{NpSa} is the best candidate to predict the structural response, it is necessary to develop more studies regarding the prediction of nonlinear seismic response because I_{NpVel} could be a good candidate in the case of high rise buildings or structures with vibration periods close to the soil period.
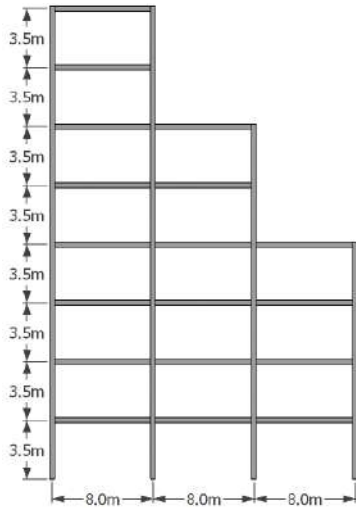
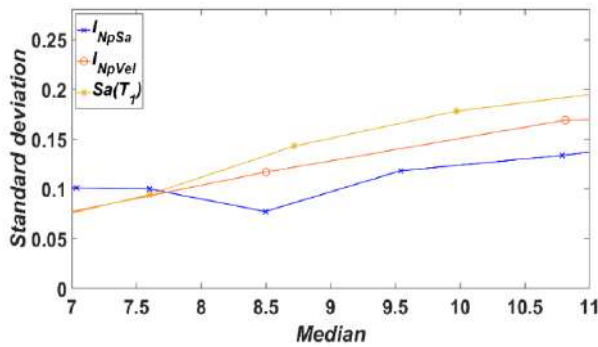Fig. 18 Geometrical characteristics of the irregular steel frame

Fig. 19 Standard deviation of the peak floor acceleration of the two cases of the generalized intensity measure I_{Npg} and $Sa(T_1)$ at different median values of the peak floor acceleration for the irregular steel frame
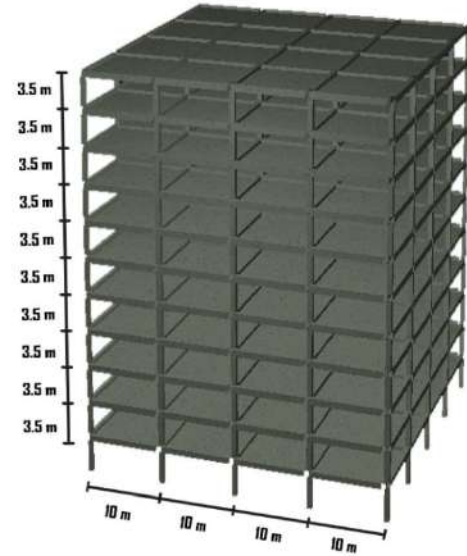

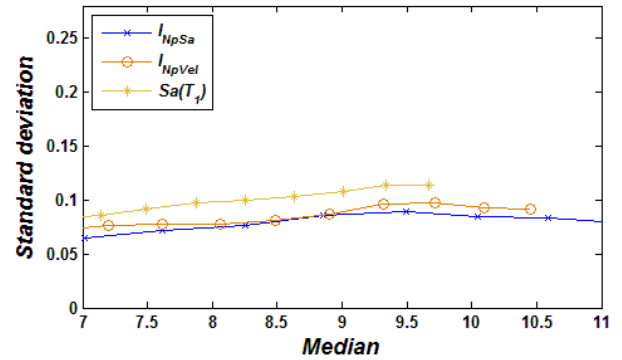Fig. 20 3D view of the reinforced concrete framed building with 15 story levels

Fig. 21 Standard deviation of the peak floor acceleration of the two cases of the generalized intensity measure I_{Npg} and $Sa(T_1)$ at different median values of the peak floor acceleration for the 3D reinforced concrete building

7. Peak floor acceleration prediction of an irregular steel frame and a 3D reinforced concrete building using acceleration and velocity spectral shape

In this section, the efficiency of the selected intensity measures to predict the response of an eight stories steel frame with vertical irregularities is computed using incremental dynamic analysis as in the case of the previous structural models. The geometrical characteristics of the structure are illustrated in Fig. 18. Fig. 19 compares the results of the standard deviation of the peak floor acceleration for the two cases of the generalized intensity measure I_{Npg} (pseudo-acceleration and velocity) and $Sa(T_1)$ at a specific median value. Notice that while the vertical axis corresponds to the standard deviation of the peak floor acceleration, the horizontal represents the median peak floor acceleration value. For the case of the irregular structure, the I_{NpSa} intensity measure is superior to predict the peak floor acceleration demands. This conclusion is also valid for the 3D reinforced concrete building with 15 story levels of Fig. 20. Notice that in this building, the story height is equals to 3.5 m and the length of the bays in both horizontal directions is equal to 10 m. Fig. 21 indicates that for the

reinforced concrete frame the standard deviation is reduced when the I_{NpSa} is selected in comparison with I_{NpVel} and $Sa(T_1)$. Finally, it is important to say that for very tall buildings which are sensitive to higher mode effects, it is recommended to use another spectral-shape-based intensity measure such as the recently proposed I_B by Bojórquez *et al.* (2017b).

8. Conclusions

In this paper, the generalized seismic intensity measure I_{Npg} was analyzed. One of the main characteristics of this seismic intensity measure is that it takes into account the non-linear behavior through the spectral shape; in addition, since it is a generalized spectral parameter, it can be defined from any type of spectrum as in the case of acceleration, velocity, displacement, input energy, inelastic parameters and so on, but in this study the spectral acceleration and velocity have been considered.

The efficiency of spectral acceleration at first mode of vibration to predict the seismic response of steel framed buildings under narrow-band motions was compared with two particular cases of the presented generalized ground motion intensity measure I_{Npg}. Although several studies have already shown the efficiency of traditional I_{Np} (here names as I_{NpSa}), the advantages of two particular cases of the generalized seismic intensity measure I_{Npg} in comparison with $Sa(T_1)$ have been observed, where the uncertainty to predict the peak floor acceleration demands of the selected structures was considerably reduced.

According to the results, it is concluded that the two particular cases of the generalized intensity measure I_{Npg} are more efficient than the traditional and most used $Sa(T_1)$; moreover, the efficiency of the intensity measure I_{NpSa} in comparison with I_{NpVel} is in general superior for different type of structural systems. Thus, the generalized ground motion intensity measure is the best option to predict peak floor accelerations in steel framed buildings and preliminary for 3D reinforced concrete buildings; however, more studies need to be conducted to select different types of spectral shapes to define I_{Npg}, especially for high rise buildings. It is important to say that for very tall buildings the I_B intensity measure could provide better results in comparison with I_{Npg}.

Acknowledgments

References

Aptikaev, F.F. (1982), "On the correlations of MM intensity with parameters of ground shaking", *The 7th European Conference on Earthquake Engineering*, Atenas, Grecia, 20-25.

Arias, A. (1970), "A measure of earthquake intensity", *Seismic Des. Nuclear Power Plants*, MIT Press, Cambridge, MA, 438-483.

Bojórquez, E. and Iervolino, I. (2011), "Spectral shape proxies and nonlinear structural response", *Soil Dyn. Earthq. Eng.*, **31**(7), 996-1008. https://doi.org/10.1016/j.soildyn.2011.03.006.

Bojórquez, E., Baca, V., Bojórquez, J., Reyes-Salazar, A., Chávez, R. and Barraza, M. (2017), "A simplified procedure to estimate peak drift demands for mid-rise steel and R/C frames under narrow-band motions in terms of the spectral-shape-based intensity measure", *Eng. Struct.*, **150**, 334-345. https://doi.org/10.1016/j.engstruct.2017.07.046.

Bojórquez, E., Chávez, R., Reyes-Salazar, A., Ruiz, S.E. and Bojórquez, J. (2017b), "A new ground motion intensity measure I_B", *Soil Dyn. Earthq. Eng.*, **99**, 97-107. https://doi.org/10.1016/j.soildyn.2017.05.011.

Bojórquez, E., Iervolino, I. and Reyes-Salazar, A. (2011), "Which spectral shape really matter to predict nonlinear structural response: application to steel frames", *Proc of 8th international conference on urban earthquake engineering* (CUEE), Tokio, Japan.

Bojórquez, E., Iervolino, I., Reyes-Salazar, A. and Ruiz, S.E. (2012), "Comparing vector-valued intensity measures for fragility analysis of steel frames in the case of narrow-band ground motions", *Eng. Struct.*, **45**, 472-480. https://doi.org/10.1016/j.engstruct.2012.07.002.

Bojórquez, E., Reyes-Salazar, A., Ruiz, S.E. and Bojórquez, J. (2013), "A new spectral shape-based record selection approach using N_p and genetic algorithms", *Mathem. Prob. Eng.*, 1-9. https://doi.org/10.1155/2013/679026.

Bojórquez, E., Reyes-Salazar, A., Terán-Gilmore, A. and Ruiz, S.E. (2010), "Energy-based damage index for steel structures", *Steel Compos. Struct.*, **10**(4), 343-360. https://doi.org/10.12989/scs.2010.10.4.331.

Bojórquez, E., Velázquez-Dimas, J., Astorga, L. Reyes-Salazar, A. and Terán-Gilmore, A. (2015), "Prediction of hysteretic energy demands in steel frames using vector-valued IMs", *Steel Compos. Struct.*, **19**(3), 697-711. https://doi.org/10.12989/scs.2015.19.3.697.

Buratti, N. (2012), "A comparison of the performances of various ground–motion intensity measures", *The 15th World Conference on Earthquake Engineering*, Lisbon, Portugal, 24-28.

Carr, A. (2011), "RUAUMOKO inelastic dynamic analysis program", Departament of Civil Engineering, University of Cantenbury, Nueva Zelanda.

Cordova, P.P., Dierlein, G.G., Mehanny, S.S.F. and Cornell, C.A. (2001), "Development of a two parameter seismic intensity measure and probabilistic assessment procedure", *The second U.S.-Japan Workshop on Performance-Based Earthquake Engineering Methodology for Reinforce Concrete Building Structures*, Sapporo, Hokkaido, 187-206.

Eads, L., Miranda, E. and Lignos, D. (2016), "Spectral shape metrics and structural collapse potential", *Earthq. Eng. Struct. Dyn.*, **45**(10), 1643-1659. https://doi.org/10.1002/eqe.2739.

Horne, P. and Burton, H. (2003), "Investigation of code seismic force levels for hospital equipment. Report ATC-29-2", *Proceedings of a seminar on seismic design*, *performance and retrofit of nonstructural components in critical facilities*, Redwood City (CA): Applied Technology Council.

Housner, G.W. (1952), "Spectrum intensities of strong motion earthquakes", *Proceedings of the symposium on earthquake and blast effects on structures*, Earthquake Engineering Research Institute.

Housner, G.W. (1975), "Measures of severity of ground shaking. U.S.", *Conference on Earthquake Engineering*, Earthquake Engineering Research Institute.

Kazantzi, A.K. and Vamvatsikos, D. (2015), "Intensity measure selection for vulnerability studies of building classes" *Earthq. Eng. Struct. Dyn.*, **44**(15), 2677-2694. https://doi.org/10.1002/eqe.2603.

Kehoe, B.E. and Freeman, S.A. (1998), "A critique of procedures for calculating seismic design forces for nonstructural elements", *Seminar on seismic design*, *retrofit*, *and performance of nonstructural components*, ATC-29-1. Redwood City (CA), Applied Technology Council.

Kostinakis, K., Athanatopoulou, A. and Morfidis, K. (2015), "Correlation between ground motion intensity measures and seismic damage of 3D R/C buildings", *Eng. Struct.*, **82**, 151-167. https://doi.org/10.1016/j.engstruct.2014.10.035.

Málaga-Chuquitaype, C. and Bougatsas, K. (2017), "Vector-IM-based alternative framing systems under bi-directional", *Eng. Struct.*, **132**(2017), 188-204. https://doi.org/10.1016/j.engstruct.2016.11.021.

Mehanny, S.S.F. (2009), "A broad-range power-law form scalar-based seismic intensity measure", *Eng. Struct.*, **31**, 1354-1368. https://doi.org/10.1016/j.engstruct.2009.02.003.

Minas, S., Galasso, C. and Rossetto, T. (2014), "Preliminary investigation on selecting optimal intensity measures for

simplified fragility analysis of mid-rise RC buildings", *2nd European Conference on Earthquake Engineering and Seismology* (2ECEES), Istanbul, Turkey, 24-29.

Modica, A. and Stafford, P. (2014), "Vector fragility surfaces for reinforced concrete frames in Europe", *Bull. Earthq. Eng.*, **12**(4), 1725-1753.

Rajabnejad, H., Hamidi, H., Naseri, S.A. and Abbaszadeh, M.A. (2021), "Effect of intensity measure on the response of a 3D-structure under different ground motion duration", *Int. J. Eng.*, **34**(10),1-19. 10.5829/IJE.2021.34.10A.04

Riddell, R. (2007), "On ground motion intensity indices", *Earthq. Spectra*, **23**(1), 147-173. https://doi.org/10.1193/1.2424748.

Shome, N. (1999), *Probabilistic Seismic Demand Analysis of Nonlinear structures*, Ph.D. Thesis, Stanford University.

Tothong, P. and Luco, N. (2007), "Probabilistic seismic demand analysis using advanced ground motion intensity measures", *Earthq. Eng. Struct. Dyn.*, **36**, 1837-1860. https://doi.org/10.1002/eqe.696.

Vamvatsikos, D. and Cornell, C.A. (2002), "Incremental dynamic analysis", *Earthq. Eng. Struct. Dyn.*, **31**, 491-514. https://doi.org/10.1002/eqe.141.

Von Thun, J.L. (1988), "Earthquake ground motions for design and analysis of dams", *Earthq. Eng. Soil Dyn. II-recent Advan. Ground-Motion Evaluat.*

Yakhchalian, M., Nicknam, A. and Amiri, G.G. (2015), "Optimal vector-valued intensity measure for seismic collapse assessment of structures", *Earthq. Eng. Eng. Vib.*, **14**(1), 37-54. https://doi.org/10.1007/s11803-015-0005-6.

CC